

NMR Relaxation Study of the Bacteriochlorophyll *c* in Solutions

Zheng-Yu Wang,* Tomoyuki Kadota, Masayuki Kobayashi, Atsuo Kasuya, and Tsunenori Nozawa

Department of Biomolecular Engineering, Graduate School of Engineering, Center for Interdisciplinary Research, Tohoku University, Sendai 980-8579, Japan

Received: June 9, 2004

Bacteriochlorophyll (BChl) *c* is a major light-harvesting pigment family in green photosynthetic bacteria. In organic solvents, the pigment molecules are capable of forming stable dimers and self-assembling into high aggregates which have been used as a model for the native chlorosome antenna. NMR relaxation times were measured for the intact farnesyl (3^1R)-[*E, E*]BChl c_F in methanol, acetone, and carbon tetrachloride. The spin–lattice relaxation times (T_1^H) were determined to be 0.3–1.2 s for the macrocyclic protons and 0.73–3.3 s for the farnesyl protons in methanol and acetone in which the BChl *c* exists as a monomer. Strong hydrogen bonding between the BChl *c* and solvent molecules resulted in a significant reduction in the spin–spin relaxation times (T_2^H) for the protons close to the hydrogen-bonding sites. This result can be interpreted in terms of a combined effect of scalar coupling with the hydroxyl proton and dipolar interaction with the solvent molecules. Formation of BChl *c* dimer in carbon tetrachloride led to an increase in T_1^H and a large decrease in T_2^H with respect to the values of monomer, indicating that the correlation time became longer as a result of the much reduced molecular motion. With the use of a highly randomly ^{13}C -labeled sample, we were able to measure the ^{13}C relaxation times. The T_1^C were determined in a range of 0.26–3.3 s for the macrocyclic carbons in methanol, and these values decreased as BChl *c* formed a dimer but remained in the same order of magnitude. The (3^1R)-[*E, E*]BChl c_F is demonstrated as an ideal molecule for studying the hydrogen-bonding property and the dynamic exchange behavior of the individual molecules within a dimer.

Introduction

Bacteriochlorophyll (BChl) *c* is a major green pigment family that occurs in green sulfur photosynthetic bacteria and constitutes about 90% of the total chlorophyll-type pigments.^{1,2} Most BChls *c* are present in chlorosome, an antenna complex with a typical size of 150–250 nm.^{3–5} They function to absorb solar energy and transfer it to the adjacent photosynthetic membrane. The absorption maximum of the native chlorosome at long wavelength (Q_y) is around 740 nm, about 70 nm red-shifted from that of the BChl *c* monomeric form as observed in polar organic solvents. Because only a small amount of protein was isolated from chlorosomes,⁶ pigment–pigment interaction has been suggested to play an essential role in the organization of the pigments in chlorosomes.^{7–10} This is also supported by the characteristic feature that BChl *c* is capable of self-association in vitro to form high aggregates in hexane with an absorption spectrum closely resembling that of native chlorosome.^{7,11,12} Many spectroscopic measurements have been made to elucidate the in vitro structure of the 740 nm aggregate in relation with the organization of BChl *c* in chlorosomes.^{7–11,13} Two functional groups, the 3^1 hydroxyl and 13^1 keto groups (Figure 1), were identified as playing key roles in ligation and hydrogen bonding in the BChl *c* aggregates. However, due to its large molecular weight and structural heterogeneity, the structure of the 740 nm aggregate has not been solved.

Beside the 740 nm high aggregate, there are several other species of BChl *c* formed in organic solvents. In nonpolar solvents, such as CCl_4 and benzene, BChl *c* shows a Q_y

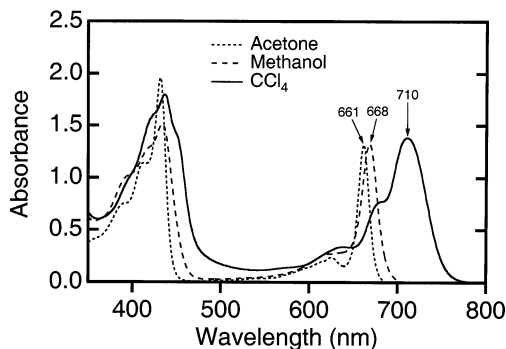
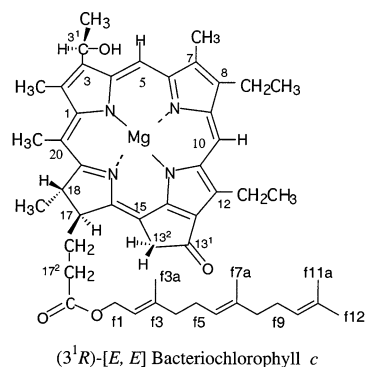


Figure 1. Molecular structure of the intact (3^1R)-[*E, E*]BChl c_F and its absorption spectra in acetone (dotted line), methanol (dashed line), and CCl_4 (solid line). The Q_y peak positions are indicated, and all spectra were normalized by the Q_y peak intensity.

absorption maximum at 710 nm (Figure 1), whereas in polar solvents, such as methanol and acetone, the Q_y absorption

* Corresponding author. Fax: +81-22-217-7278. E-mail: wang@biophys.che.tohoku.ac.jp.

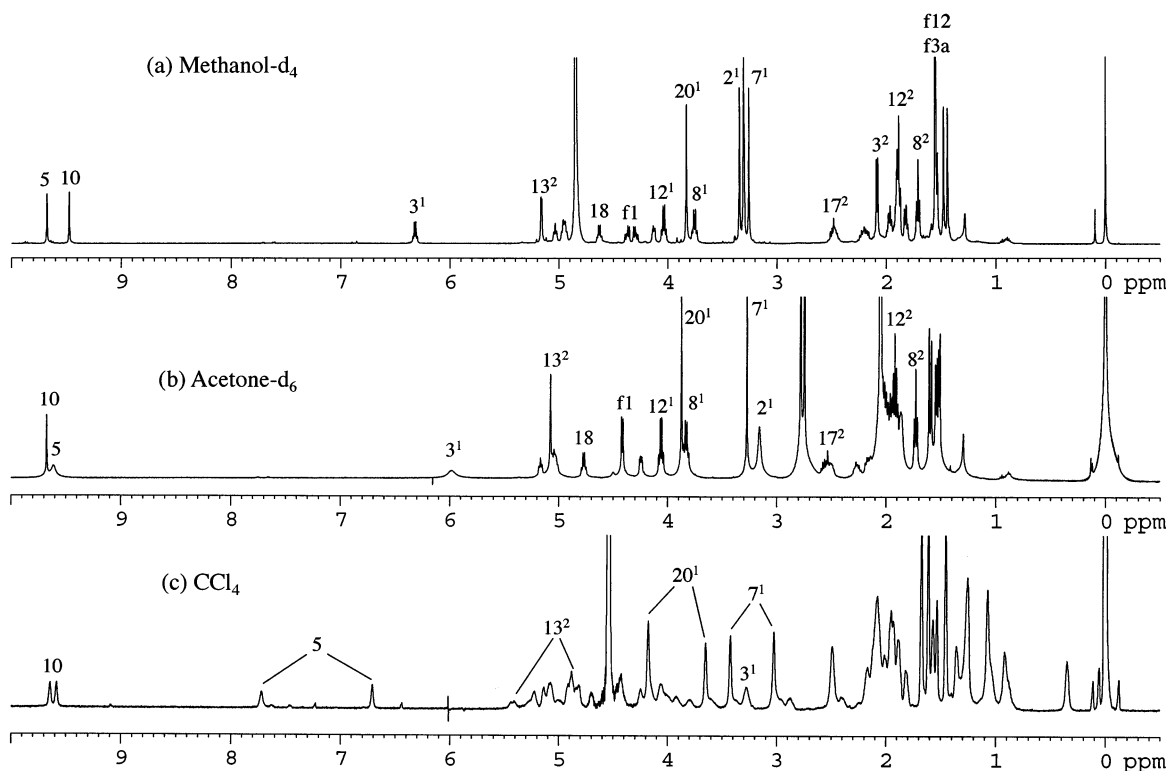


Figure 2. ^1H NMR spectra of the (3^1R) -[*E, E*]BChl c_F in methanol- d_4 (top), acetone- d_6 (middle), and CCl_4 (bottom). Only parts of the assignments are indicated. All assignments were made on the basis of ^1H - ^{13}C heteronuclear multiple-quantum coherence spectra. See ref 14 for the details.

maxima appear between 660 and 670 nm. The 710 nm species was identified by a small-angle neutron scattering experiment as being dominated by highly stable BChl *c* dimers.¹⁴ The dimer structure formed in CCl_4 at room temperature has been precisely determined to have an antiparallel “piggy-back” conformation by ^1H , ^{13}C , and ^{15}N NMR spectroscopies.^{15,16} All these NMR spectra are characterized by two asymmetric resonances resolved for each type of the individual functional groups, indicating that the two molecules in the dimer experience slow exchange between two nonequivalent configurations. The exchange rate constants were evaluated within a range of 0.03–0.48 s^{-1} depending on the solvent and temperature.^{17,18}

In this work, we further explore the dynamic properties of BChl *c* in terms of relaxation behavior by measuring the NMR spin–lattice relaxation times (T_1) and spin–spin relaxation times (T_2) in different organic solvents. The results of this study not only provide an alternative explanation of the exchange phenomenon on the basis of molecular motion but also provide an important clue to the interpretation of the different spectral appearance observed in different solvents. For example, as shown in Figure 2, although the BChl *c* molecule exists as a monomer in both methanol and acetone, two meso protons (5-H and 10-H) exhibited the same spectral shape in methanol, but the 5-H proton gave rise to a much broadened peak in acetone, whereas the spectral shape of 10-H proton remained unchanged. A similar behavior was also observed for the 3^1-H and 2^1-H signals. When BChl *c* formed dimers in CCl_4 solution a completely different spectrum was obtained with increased spectral widths for all resonances. Although there exist a number of NMR relaxation studies on the synthetic porphyrins and related compounds in the literature,^{19–22} only limited information is available on the relaxation properties of the naturally occurring (bacterio)chlorophylls.^{23,24} In addition, the investigation of relaxation properties of chlorophyll dimers has been limited to the samples that undergo fast exchange between the monomer

and dimer species.^{24–26} Hence, the relaxation times were actually measured on the averaged resonances arising from various species. Because the exchange rate of BChl *c* dimers in CCl_4 is slow enough at room temperature to allow observation of two distinct resonances for each type of the functional group, we were able to precisely evaluate and compare the relaxation behavior of individual functional groups in different environments within the dimer. Such information is useful in examining the mechanism of photoinduced energy transfer of antenna complex in terms of the internal motion of the pigment molecules.

Experimental Section

Materials and Sample Preparation. Crude BChl *c* mixtures were extracted from dry cells of thermophilic green sulfur photosynthetic bacterium *Chlorobium tepidum* with methanol, and the major component (3^1R) -[*E, E*]BChl c_F (8,12-diethyl BChl *c* esterified with farnesol) was then purified by chromatography as described elsewhere.^{8,9} Partially ^{13}C -enriched samples were obtained with a medium containing sodium acetate- $1\text{-}^{13}\text{C}$ ($^{13}\text{C} > 99.9\%$ atom, Isotec Inc.) and natural abundance NaHCO_3 . This medium resulted in a highly randomly ^{13}C -labeled (3^1R) -[*E, E*]BChl c_F (hereafter referred to as the fractionally ^{13}C -enriched sample). The average enrichment factor was estimated to be less than 40% based on ^1H NMR integration of the 3^1-H signals.^{15,16} Deuterated methanol (CD_3OD , $D > 99.95\%$ atom) and deuterated acetone (CD_3COCD_3 , $D > 99.9\%$ atom) were from Merck (Darmstadt, Germany) and Isotec Inc. (Miami, OH), respectively. Carbon tetrachloride (purity $> 99.8\%$, Infinity pure grade) was purchased from Wako Pure Chemical Industries, Ltd. (Japan) and was dried with Na_2CO_3 during storage. Pigments and solvents were degassed separately and then purged with argon gas. BChl *c* solutions were prepared under argon atmosphere by dissolving the dried pigments in solvents to a monomer concentration of 1.5 mM. The solutions

were then moved into NMR tubes and further purged with argon gas before the NMR tubes were sealed.

NMR Measurements and Relaxation Time Analysis. All NMR experiments were conducted on a Bruker DRX-500 spectrometer at 298 K. Field–frequency lock for the sample in pure CCl₄ solution was achieved by inserting a 1 mm D₂O-filled inner tube in the 5 mm NMR tubes. Longitudinal relaxation times T_1 were recorded using the inverse-recovery (180°– t –90°) method. For the ¹³C measurements, power-gated decoupling was used during the acquisition period. Transverse relaxation times T_2 were measured by the Carr–Purcell–Meiboom–Gill spin–echo method. Relaxation times were calculated by fitting seven data points with eqs 1 and 2

$$I = A + B \exp(-t/T_1) \quad (1)$$

$$I = C \exp(-t/T_2) \quad (2)$$

where A , B , and C are constants and I is the peak intensity for the spectrum obtained at time t . Relaxation delays between acquisitions were taken at least 10 times the longest T_1 or T_2 of interest. Correlation times τ_c , defined as the average length of time that the molecule can be considered to stay in a particular state of motion, were estimated using the Debye theory of dielectric dispersion²⁷

$$\tau_c = 4\pi\eta a^3/3kT \quad (3)$$

where η is the viscosity of the solution and a is the effective radius of the molecule.

The correlation time can be related to relaxation times using the established macroscopic equations for the spin–lattice and spin–spin relaxations. The relaxation mechanisms generally include dipole–dipole, chemical shift anisotropy, spin–rotation interaction, and scalar coupling. In practice, the dipole–dipole interaction is often the dominant mechanism, which is also the case for the BChl *c* molecule of this study as shown in the Results and the Discussion. For a rigid, isotropically tumbling molecule, the relaxation times through the dipolar coupling are given by²⁸

$$1/T_1^H = \gamma_H^4 (h/2\pi)^2 r^{-6} (9/8) [J_1(\omega_H) + J_2(2\omega_H)] \quad (4)$$

$$1/T_2^H = \gamma_H^4 (h/2\pi)^2 r^{-6} (3/4) [(3/8)J_0(0) + (15/4)J_1(\omega_H) + (3/8)J_2(2\omega_H)] \quad (5)$$

$$1/T_1^C = (\gamma_H\gamma_C h/2\pi)^2 r^{-6} (3/4) [(1/12)J_0(\omega_C - \omega_H) + (3/2)J_1(\omega_C) + (3/4)J_2(\omega_C + \omega_H)] \quad (6)$$

where γ_H and γ_C are the magnetogyric ratios of hydrogen and carbon, h is the Planck constant, r is the internuclear distance, ω_H and ω_C are the Larmor frequencies of hydrogen and carbon, and the $J(\omega)$ are spectral density functions which can be expressed by

$$J_q(\omega) = C_q [\tau_c / (1 + \omega^2\tau_c^2)] \quad (q = 0, 1, 2) \quad (7)$$

where $C_0 = 24/15$, $C_1 = 4/15$, and $C_2 = 16/15$.

Results

¹H NMR Relaxation Behavior. BChl *c* molecules are known to exist as monomers in both methanol and acetone solutions.^{9,29} However, the ¹H NMR spectra of (3¹R)-[*E, E*]BChl *c*_F in the two solvents revealed a marked difference in the spectral shape

(Figure 2). To clarify the reason, relaxation times T_1^H and T_2^H were measured for all protons of the (3¹R)-[*E, E*]BChl *c*_F, and the results are shown in Table 1. In methanol, macrocyclic protons exhibited T_1^H over a range of 0.36–1.2 s and T_2^H over a range of 0.19–0.74 s. Two meso protons had the same, relatively large T_1^H values compared to most other side chain protons. The methyl protons of the side chains showed longer T_1^H and T_2^H than the methylene protons and the protons directly attached to the macrocycle (i.e., 8²-H vs 8¹-H, 12²-H vs 12¹-H, and 18¹-H vs 18-H), indicating that the protons located farther from the macrocycle are more mobile than those of directly attached functional groups. The only exception was observed for the protons of the propionic side chain, where 17¹-H and 17²-H showed smaller values for T_1^H and T_2^H than 17-H. This may be explained by both a hydrogen-bond formation between the carboxyl of the (3¹R)-[*E, E*]BChl *c*_F and hydroxyl group of methanol and a conformational constraint as indicated in a previous study¹⁵ because this part serves as a linker between the macrocycle and the long farnesyl chain. It is also evident that f1-H has a much smaller T_1^H than other farnesyl protons. The shortest T_2^H (0.19 s) was observed for 13²-H in methanol. This again may be attributed to a hydrogen bonding between the neighboring 13¹ carbonyl and hydroxyl group of methanol (see below).

For all protons, the spin–lattice relaxation times T_1^H measured in acetone are in the same order of magnitude as those measured in methanol with typical ratios of T_1^H (acetone) to T_1^H (methanol) in a range of 1.10–1.25. However, the spin–spin relaxation times T_2^H revealed large variation in acetone (Table 1). Especially, 2¹-H, 3¹-H, and 5-H exhibited extremely small T_2^H values with respect to other protons. We were not able to measure the relaxation times for 3²-H due to the signal overlap with the strong peak of the residual undeuterated acetone of the solvent. Figure 3 illustrates a schematic map of the ratio of T_2^H (acetone) to T_2^H (methanol) for the macrocyclic protons. The protons around 3¹-C had T_2^H values about 1 order of magnitude smaller than those measured in methanol. This result indicates that formation of the hydrogen bond between the 3¹-OH and the carbonyl of acetone drastically reduces the T_2^H of the surrounding protons but with little effect on their T_1^H . Farnesyl protons had similar values for the relaxation times in both methanol and acetone solutions. Hence, there is no significant change in the molecular motion of this long chain when the BChl *c* is dissolved as a monomer in the two solvents.

BChl *c* forms dimers in CCl₄, with a slow exchange between the two nonequivalent configurations. As a result, each type of proton gave rise to two resonances, causing substantial overlap of the signals (Figure 2). Although all resonances can be identified and assigned by two-dimensional heteronuclear correlation spectra,¹⁵ it was difficult to measure the relaxation times for some of the protons whose signals heavily overlapped with others. For this reason, we only listed the values in Table 1 for the protons whose T_1^H and T_2^H can be reliably evaluated. Most macrocyclic protons exhibited larger T_1^H values in CCl₄ by a factor of 1.2–1.8 compared to those in methanol and acetone. In contrast, the T_2^H values decreased drastically for all protons as the BChl *c* dimer formed in CCl₄. This can also be confirmed by the observation of increased line broadening in the spectrum (Figure 2). The results indicate that T_2^H is much more sensitive than T_1^H to molecular aggregation and exchange. A similar phenomenon was also observed for the pyrrole protons of a porphyrin-linked peptide in methanol–aqueous solution.²² Another feature of the BChl *c* dimer of this study is that some protons of the same type but belonging to different molecules

TABLE 1: ^1H NMR Relaxation Times of (3^1R)-[*E, E*]BChl c_F in Methanol- d_4 , Acetone- d_6 , and CCl_4 at Room Temperature

position	T_1^{H} [s]			T_2^{H} [s]		
	CD_3OD	$(\text{CD}_3)_2\text{CO}$	CCl_4	CD_3OD	$(\text{CD}_3)_2\text{CO}$	CCl_4
2 ¹ -H	0.59	0.69	0.94, 0.94	0.37	0.035	0.10
3 ¹ -CH	0.75	0.80	1.1, 0.98	0.42	0.054	0.050
3 ² -H	0.54	0.77	0.64, 0.49	0.42		0.050
5-H	0.89	0.98	1.4, 1.4	0.39	0.027	0.061, 0.085
7 ¹ -H	0.71	0.81	1.3, 1.3	0.39	0.53	0.090, 0.074
8 ¹ -H	0.39	0.46		0.31	0.39	
8 ² -H	0.73	0.84		0.49	0.56	
10-H	0.89	1.1	1.2, 1.2	0.37	0.57	0.092, 0.11
12 ¹ -H	0.71	0.99	1.2, 1.3	0.38	0.76	0.074, 0.071
12 ² -H	1.2	1.7		0.74	1.2	
13 ² -H	0.39	0.48	0.82	0.19	0.32	
17-H	0.72	0.87	0.76	0.36	0.35	0.11
17 ¹ -H	0.37	0.39		0.31	0.25	
17 ² -H	0.36	0.44	0.93, 1.0	0.28	0.26	
18-H	0.58	0.65	0.90	0.29	0.44	0.081
18 ¹ -H	0.61	0.75	0.74, 0.82	0.30	0.46	0.062, 0.13
20 ¹ -H	0.57	0.66	1.2, 1.1	0.26	0.40	0.068, 0.073
f1-H	0.73	0.99		0.55	0.67	
f2-H	1.6	2.1	1.3, (1.3–1.5) ^a	0.70	0.57	(0.27–0.29) ^a
f3a-H		2.0	1.4	1.4	0.28	
f4-H	1.3	1.5	0.9	0.89	1.0	0.36
f5-H	0.91	(1.3–1.9) ^a		0.68	(1.4–2.2)	
f6-H	1.9	2.2	1.4, (1.3–1.5) ^a	0.47		(0.27–0.29) ^a
f7a-H	1.9	2.5	1.6	1.5	2.2	0.71
f8-H	1.2	1.6	0.9	0.52	1.0	0.36
f9-H	1.2	(1.3–1.9) ^a		0.71	(1.4–2.2) ^a	
f10-H	3.3	2.5	(1.3–1.5) ^a	0.64		(0.27–0.29) ^a
f11a-H	2.7	2.8		2.1	3.0	
f12-H	1.4	2.3	1.2	1.1	2.0	0.65

^a The values in the parentheses are provisional.

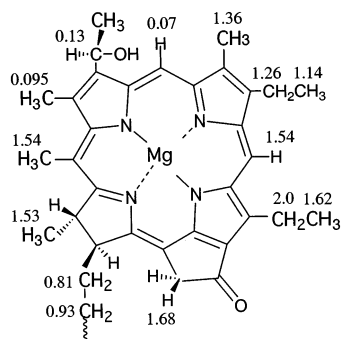


Figure 3. Schematic map showing the ratio of T_2^{H} in acetone to T_2^{H} in methanol for the protons of the (3^1R)-[*E, E*]BChl c_F macrocycle. Extremely small ratios were observed for the protons around the 3¹ hydroxyl group, and relatively large ratios were observed for the protons around the 13¹ carbonyl groups.

in the dimer revealed different relaxation behavior. For example, the two 5-H protons in the dimer showed identical T_1^{H} but had different T_2^{H} , and two 18-H protons showed different values for both T_1^{H} and T_2^{H} . This feature may be related to the asymmetric structure of the dimer. The farnesyl protons in CCl_4 also showed much smaller T_2^{H} . This is in agreement with a previous observation that the long side chain is in a highly restricted motion in the dimer and may adopt a folding-back conformation with most portion of the chain fluctuating around the periphery of the macrocycle.¹⁵

^{13}C NMR Relaxation Behavior. So far, little is known about the ^{13}C NMR relaxation times of (bacterio)chlorophylls due to the low natural abundance and low sensitivity for the ^{13}C nucleus. Most studies using ^{13}C enrichment technique have been devoted to the assignment of resonances and elucidation of the molecular structures of these compounds.^{16,30,31} The fractionally ^{13}C -enriched BChl *c* of this study enables us to measure the

TABLE 2: ^{13}C Spin–Lattice Relaxation Times (T_1^{C}) of (3^1R)-[*E, E*]BChl c_F in Methanol- d_4 and CCl_4 at Room Temperature

position	CD_3OD [s]	CCl_4 [s]
2-C		0.93, 0.95
2 ¹ -CH ₃	1.2	0.69, 0.92
3 ¹ -CH	0.46	0.20, 0.26
3 ² -CH ₃	0.68	0.27, 0.33
7-C		0.90, 1.2
7 ¹ -CH ₃	1.5	1.3, 1.4
8 ¹ -CH ₂	0.31	
8 ² -CH ₃	1.1	0.74, 0.8
12-C	2.8	1.1
12 ¹ -CH ₂	1.8	
12 ² -CH ₃	1.8	0.86, 0.98
13 ¹ -C=O	3.3	1.1, 0.82
13 ² -CH ₂	0.30	
17 ¹ -CH ₂	0.26	
17 ² -CH ₂	0.38	0.21
17 ³ -C(O)	3.0	1.4
18-CH ₃	0.39	0.26, 0.28
18 ¹ -CH ₃	0.68	0.47, 0.51
20 ¹ -CH ₃	1.1	0.88, 1.1
f1-CH ₂	0.54	0.54
f2-CH	1.5	0.56, 0.64
f3-C	7.4	1.8, 2.2
f3a-CH ₃		1.4, 1.5
f5-CH ₂	1.1	0.95, 1.0
f7-C	6.1	
f9-CH ₂	1.8	0.6, 0.7

^{13}C spin–lattice relaxation time T_1^{C} , and the result is shown in Table 2. As described in a previous study,¹⁶ the labeling pattern using the mixed carbon source ($\text{CH}_3^{13}\text{COONa}$ and NaHCO_3) in the medium revealed that macrocyclic carbons 9-C, 14-C, 16-C, as well as all meso carbons, were specifically unlabeled. The 3-C, 4-C, 8-C, and 13-C carbons were only slightly enriched and failed to give observable NMR signals.^{16,32} In methanol,

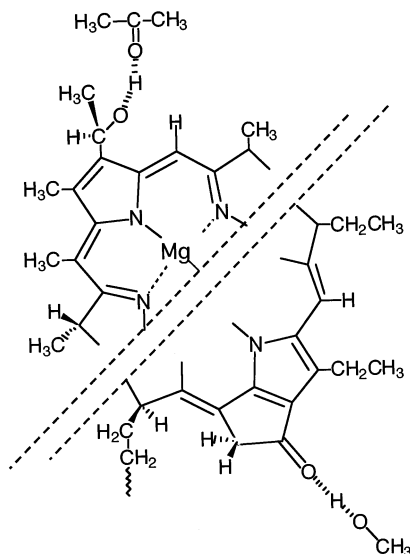


Figure 4. Schematic illustration showing the hydrogen bondings between the 3^1 hydroxyl group of the (3^1R) -[*E, E*]BChl c_F and the carbonyl of acetone (top half) and between the 13^1 carbonyl of the (3^1R) -[*E, E*]BChl c_F and the hydroxyl of methanol (bottom half).

carbonyl and carboxyl carbons showed the longest T_1^C among the observed macrocyclic carbons, followed by most methyl carbons that directly attached to the macrocycle (2^1 -C, 7^1 -C, 12^1 -C, and 20^1 -C). Large T_1^C values were also observed for the 12^2 and 8^2 methyl carbons. The quaternary carbons ($f3$ -C and $f7$ -C) of the farnesyl chain exhibited extremely long relaxation times in methanol. Similar to the proton, the ^{13}C NMR spectrum of BChl *c* in CCl_4 was characterized by two sets of resonances.¹⁶ The spin–lattice relaxation times of all carbons decreased significantly as BChl *c* formed the dimer. The BChl *c* dimer had T_1^C values between 0.2 and 1.4 s for the macrocyclic carbons and 0.54 and 2.2 s for the farnesyl carbons, respectively. Different T_1^C values were observed for the two resonances of most corresponding carbons.

Discussion

In this study, NMR relaxation times were measured for the intact (3^1R) -[*E, E*]BChl c_F in different organic solvents. Although BChl *c* exists in monomeric form in both methanol and acetone, almost all protons showed smaller T_1^H values in methanol. This may be partly attributed to the difference in viscosity between the two solvents: the coefficient of viscosity of the methanol is much larger than that of acetone (0.59 cP vs 0.32 cP at 20 °C). A greater viscosity corresponds to a longer correlation time τ_c as shown in eq 3 and consequently results in a shorter T_1 if the solution system is under the “extreme narrowing condition”, which is considered the case for the BChl *c* monomers in methanol and acetone. The relaxation times may also be affected by ligation state, as it is known that BChl *c* forms a pentacoordinated complex with one axial ligand in acetone and other nonpolar solvents, whereas the central Mg is hexacoordinated by two axial ligands in methanol and pyridine, as derived from the results of resonance Raman, absorption, CD, and magnetic CD.^{29,33}

Most protons had smaller T_2^H values in methanol compared with acetone. However, extremely short T_2^H were observed for 2^1 -H, 3^1 -H, and 5 -H in acetone (Table 1) as evidenced from their broad line widths (Figure 2b). This result can be exclusively explained by a strong hydrogen bond formation between the pigment’s 3^1 -OH and the C=O groups of acetone (Figure 4).

Hydrogen bonding decreases the rate of intermolecular proton exchange, and the hydroxyl proton remains bonded for a sufficient time to exert its spin coupling. The reduced exchange rate leads to a broadening of the coupled proton signals and enables us to observe the resonances from hydroxyl protons which otherwise would disappear due to fast exchange. The method of using a strong hydrogen bond acceptor solvent, such as acetone and dimethyl sulfoxide, is often employed as a useful diagnostic procedure for characterizing the OH and coupled hydrogen signals even in dilute solution. In a previous NMR study¹⁵ on the BChl *c* dimer in CCl_4 , we observed a 1H resonance at 4.46 ppm and provisionally assigned it to the 3^1 -OH. There was also a small broad peak observed at 4.50 ppm for the (3^1R) -[*E, E*]BChl c_F in acetone as shown in Figure 2c, which might arise from the 3^1 hydroxyl proton. In general, the influence of scalar coupling due to hydrogen bonding is limited to closely connected functional groups through the chemical bonds. In the present study, this can account for the increase in the line width of 3^1 -H but can hardly interpret the line broadening of 5 -H and 2^1 -H. Another cause of broadening of NMR spectral lines that is usually more important is the so-called “dipolar” broadening,²⁷ which is the dominant broadening factor in organic solids. The presence of a group of spins around a given spin may result in a number of interactions. The most important interaction between the spin and its surrounding spins is the dipolar interaction. It could be homonuclear or heteronuclear dipolar coupling. We only consider here the proton (homonuclear) dipolar coupling, and in this case the effect of spin–spin exchange, related to T_2^H , needs to be taken into account. As a result, the interactions between the hydrogen-bonded acetone and the protons around the 3^1 group of the BChl *c* are considered to make the major contribution to the extremely small T_2^H values for the 5 -H and 2^1 -H signals. Similar interactions due to the hydrogen bonding should also occur for the protons around the 13^1 carbonyl (Figure 4), and in fact relatively short T_2^H were observed for the 13^2 -H, 12^1 -H, and 12^2 -H in methanol as compared to the T_2^H in acetone.

As described above, the BChl *c* molecule provides an ideal system for studying the hydrogen-bonding property as it bears both hydroxyl and carbonyl groups. This structural feature is also responsible for its unique property of forming a stable dimer or large aggregate in nonpolar solvents. For the dimer formed in CCl_4 , the hydroxyl group is arranged in such a way that the 3^1 proton lies in the same plane as the macrocycle, the 3^1 hydroxyl group orients toward the central Mg of the adjacent molecule as a ligand, and the 3^2 methyl points to the outside of the dimer.¹⁵ As a result, the 3-hydroxyethyl, 5 -H, and 2^1 methyl groups lie over the macrocycle of the adjacent molecule as evidenced by the ring-current induced shifts.¹⁵

The dimer formation brought about significant changes in the relaxation times as shown in Tables 1 and 2. For most macrocyclic protons, the T_1^H increased markedly while the T_2^H decreased drastically compared to the corresponding relaxation times of the monomer. The result of this study can be interpreted by the dipole–dipole interaction model as described by eqs 4–6. Figure 5 shows the relationships between the relaxation times and correlation time calculated for the macrocyclic protons and carbons at $\omega_H = 500$ MHz and $\omega_C = 125$ MHz. The correlation time, as shown in eq 3, is determined by the viscosity of the solvent and the size of the molecule. The viscosity of CCl_4 (0.97 cP at 20 °C) is much higher than those of methanol (0.59 cP) and acetone (0.32 cP), and the effective radii can be evaluated from a small-angle neutron scattering experiment,¹⁴ showing that radii of gyration were 17 Å and 10 Å for the BChl *c* dimer

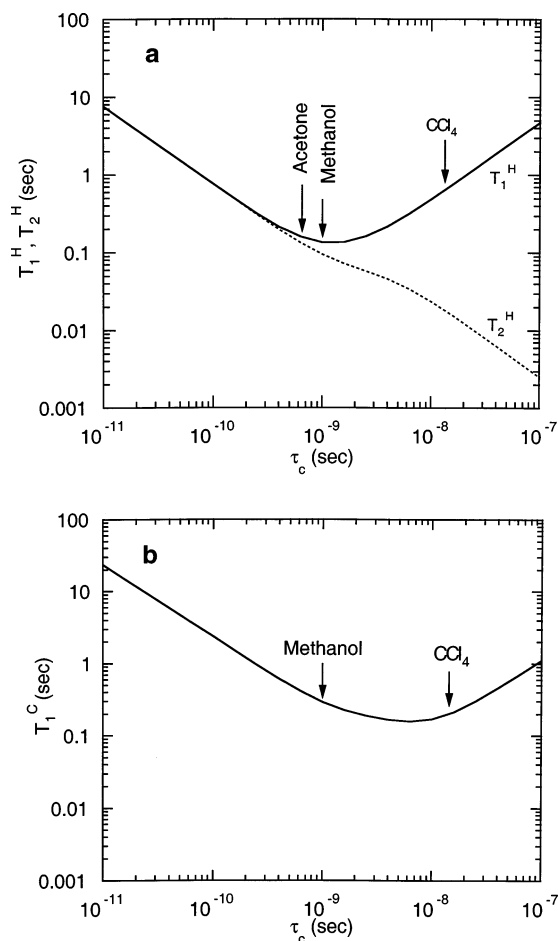


Figure 5. Relationships between the relaxation times and correlation time calculated for the macrocyclic protons and carbons using the eq 4–6. The solvents in which the (3^1R) -[*E, E*]BChl c_F are dissolved are indicated to correspond to the correlation times. (a) T_1^H (solid line) and T_2^H (dotted line) vs τ_c at $\omega_H = 500$ MHz. (b) T_1^C vs τ_c at $\omega_C = 125$ MHz.

and monomer, respectively. With the use of these parameters and eq 3, the correlation times τ_c were estimated to be 1.0×10^{-9} s, 5.9×10^{-10} s (monomers), and 1.5×10^{-8} s (dimers) for the (3^1R) -[*E, E*]BChl c_F in methanol, acetone, and CCl_4 , respectively. These values are indicated in Figure 5. In good agreement with the experiment results, T_1^H was shown to first decrease as τ_c increases in the short τ_c region with essentially the same value as T_2^H , then to reach a minimum around $\tau_c = 1.0 \times 10^{-9}$ s for the proton resonance frequency, and finally T_1^H turns to increase with τ_c in the $\tau_c > 1.0 \times 10^{-9}$ s region. In contrast, T_2^H continuously decreases as τ_c increases over the whole range of τ_c . Several characteristic features of the measured relaxation times can be reproduced from the calculation results: (1) the T_1^H measured in acetone are only slightly larger than those in methanol; (2) the values of T_1^H measured in acetone and methanol are larger than those of the corresponding T_2^H ; (3) the T_1^H measured in CCl_4 are much larger than the T_2^H and are also larger than the T_1^H in methanol and acetone. The calculated T_1^C shows a broad minimum around $\tau_c = 10^{-9}$ s and 10^{-8} s (Figure 5b), in consistent with the observed T_1^C that have the same order of magnitude for both methanol and CCl_4 . Therefore, BChl *c* in acetone can be considered to be in the fast motion regime while the BChl *c* dimer is in a much restricted motion mode in CCl_4 where the “extreme narrowing” condition no longer applies. The result is consistent with the

observation that individual BChl *c* molecules in the dimer undergo extremely slow exchange between the two nonequivalent configurations with an exchange rate constant of about 1.8 s^{-1} .^{16,18} For Chl *a* dimers, the exchange seems to be much faster, and usually only one NMR signal is observed for each functional group.^{24,34} Relaxation measurement for a limited number of protons revealed that the T_1^H of Chl *a* dimer formed in chloroform were much smaller than those of Chl *a* monomer in acetone.²⁴

Conclusions

Spin–lattice and spin–spin relaxation times were measured for the intact (3^1R) -[*E, E*]BChl c_F in different organic solvents in which the molecule exists in either monomeric or dimeric form. The T_1^H were in ranges of 0.36–1.2 s for the macrocyclic protons and 0.73–3.3 s for the farnesyl protons in methanol and acetone. The values are slightly larger than those reported for iron(III) porphyrin–imidazole complexes²⁰ but smaller than those of a porphyrin conjugate linked with an acyclic polypeptide.²² The T_2^H showed similar values to T_1^H for most protons but was found to be strongly sensitive to the hydrogen bonding. Significant reduction in the T_2^H was observed for the protons near the hydrogen-bonding site and can be rationalized by a combined effect of scalar coupling with the hydroxyl proton and dipolar interaction with the solvent molecules. Formation of (3^1R) -[*E, E*]BChl c_F dimer in CCl_4 led to an increased correlation time as a result of much reduced molecular motion. The T_1^C were in a range of 0.26–3.3 s for the macrocyclic carbons in methanol and decreased as BChl *c* formed the dimer but remained within the same order of magnitude. The T_1^C values were comparable with those observed for the iron(III)-, cobalt(III)-, and zinc(II)-porphyrins.^{19–21} The results of this work provide useful information on the dynamic properties of the stable BChl *c* dimer and can be used as quantitative measures for evaluating the internal motion of other chlorophyll-related pigment molecules.

Acknowledgment. This work was supported by Grants-in-aid for Scientific Research (Nos. 12450341, 12878108, 15350096) and the COE Project of Giant Molecules and Complex Systems, the Ministry of Education, Science, Sports and Culture, Japan, and Takeda Science Foundation.

References and Notes

- (1) Scheer, H. The Pigments. In *Light-Harvesting Antennas in Photosynthesis*; Green, B. R., Parson, W. W., Eds.; Kluwer Academic Publishers: Dordrecht, 2003; pp 29–81.
- (2) Blankenship, R. E.; Matsuura, K. Antenna Complexes from Green Photosynthetic Bacteria. In *Light-Harvesting Antennas in Photosynthesis*; Green, B. R., Parson, W. W., Eds.; Kluwer Academic Publishers: Dordrecht, 2003; pp 195–217.
- (3) Wang, Z.-Y.; Marx, G.; Umetsu, M.; Kobayashi, M.; Nozawa, T. *Biochim. Biophys. Acta* **1995**, *1232*, 187–196.
- (4) Zhu, Y.; Ramakrishna, B. L.; van Noort, P. I.; Blankenship, R. E. *Biochim. Biophys. Acta* **1995**, *1232*, 197–207.
- (5) Martinez-Planells, A.; Arellano, J. B.; Borrego, C. M.; Lopez-Iglesias, C.; Gich, F.; Garcia-Gill, J. *Photosynth. Res.* **2002**, *71*, 83–90.
- (6) Chung, S.; Frank, G.; Zuber, H.; Bryant, B. A. *Photosynth. Res.* **1994**, *41*, 261–275.
- (7) Brune, D. C.; Nozawa, T.; Blankenship, R. E. *Biochemistry* **1987**, *26* (6), 8644–8654.
- (8) Nozawa, T.; Ohotomo, K.; Suzuki, M.; Morishita, Y.; Madigan, M. T. *Bull. Chem. Soc. Jpn.* **1993**, *66*, 231–237.
- (9) Nozawa, T.; Ohotomo, K.; Suzuki, M.; Nakagawa, Y.; Shimada, Y.; Konami, H.; Wang, Z.-Y. *Photosynth. Res.* **1994**, *41*, 211–223.
- (10) Chiefari, J.; Griebenow, K.; Griebenow, N.; Balaban, T. S.; Holzwarth, A. R.; Schaffner, K. *J. Phys. Chem.* **1995**, *99*, 1357–1365.
- (11) Bystrova, M. I.; Mal'gosheva, I. N.; Krasnovskii, A. A. *Mol. Biol.* **1979**, *13*, 440–451.

- (12) Smith, K. M.; Kehres, L. A.; Fajer, J. J. *J. Am. Chem. Soc.* **1983**, *105*, 1387–1389.
- (13) Balaban, T. S.; Holzwarth, A. R.; Schaffner, K.; Boender, G.-J.; de Groot, H. J. M. *Biochemistry* **1995**, *34*, 15259–15266.
- (14) Wang, Z.-Y.; Umetsu, M.; Yoza, K.; Kobayashi, M.; Imai, M.; Matsushita, Y.; Niimura, N.; Nozawa, T. *Biochim. Biophys. Acta* **1997**, *1320*, 73–82.
- (15) Wang, Z.-Y.; Umetsu, M.; Kobayashi, M.; Nozawa, T. *J. Phys. Chem. B* **1999**, *103*, 3742–3753.
- (16) Wang, Z.-Y.; Umetsu, M.; Kobayashi, M.; Nozawa, T. *J. Am. Chem. Soc.* **1999**, *121*, 9363–9369.
- (17) Umetsu, M.; Seki, R.; Wang, Z.-Y.; Kumagai, I.; Nozawa, T. *J. Phys. Chem. B* **2002**, *106*, 3987–3995.
- (18) Umetsu, M.; Seki, R.; Kadota, T.; Wang, Z.-Y.; Nozawa, T. *J. Phys. Chem. B* **2003**, *107*, 9876–9882.
- (19) Cassidei, L.; Bang, H.; Edwards, J. O.; Lawler, R. G. *J. Phys. Chem.* **1991**, *95*, 7186–7188.
- (20) Yamamoto, Y.; Nanai, N.; Chujo, R. *Bull. Chem. Soc. Jpn.* **1991**, *64*, 3199–3201.
- (21) Noss, L.; Liddell, P. A.; Moore, A. L.; Moore, T. A.; Gust, D. J. *J. Phys. Chem. B* **1997**, *101*, 458–465.
- (22) Arai, T.; Inudo, M.; Ishimatsu, T.; Akamatsu, C.; Tokusaki, Y.; Sasaki, T.; Nishino, N. *J. Org. Chem.* **2003**, *68*, 5540–5549.
- (23) Sanders, J. K. M.; Waterton, J. C.; Denniss, I. S. *J. Chem. Soc., Perkin Trans. 1* **1978**, 1150–1157.
- (24) Kooyman, R. P. H.; Schaafsma, T. J. *J. Am. Chem. Soc.* **1984**, *106*, 551–557.
- (25) Katz, J. J.; Strain, H. H.; Leussing, D. L.; Dougherty, R. C. *J. Am. Chem. Soc.* **1968**, *90*, 784–791.
- (26) Ballschmiter, K.; Katz, J. J. *J. Am. Chem. Soc.* **1969**, *91*, 2661–2667.
- (27) Bovey, F. A. *Nuclear Magnetic Resonance Spectroscopy*, 2nd ed.; Academic Press: San Diego, CA, 1988; Chapter 1.
- (28) Abragam, A. *The Principles of Nuclear Magnetism*; Clarendon Press: Oxford, 1961; Chapter 8.
- (29) Nozawa, T.; Noguchi, T.; Tasumi, M. *J. Biochem.* **1990**, *108*, 737–740.
- (30) Boxer, S. G.; Closs, G. L.; Katz, J. J. *J. Am. Chem. Soc.* **1974**, *96*, 7058–7066.
- (31) Okazaki, T.; Kajiwara, M. *Chem. Pharm. Bull.* **1995**, *43*, 1311–1317.
- (32) Oh-hama, T.; Seto, H.; Miyachi, S. *Arch. Biochem. Biophys.* **1986**, *246*, 192–198.
- (33) Umetsu, M.; Wang, Z.-Y.; Kobayashi, M.; Nozawa, T. *Biochim. Biophys. Acta* **1999**, *1410*, 19–31.
- (34) Katz, J. J.; Janson, T. R.; Kostka, A. G.; Uphaus, R. A.; Closs, G. L. *J. Am. Chem. Soc.* **1972**, *94*, 2883–2885.